Progress In Electromagnetics Research C, Vol. 114, 203–216, 2021

Energy Harvesting System Using Rectenna Applied to Wireless Powered Remote Temperature Sensing

Felipe Zanon[1], Ursula Resende[1], Guilherme Brandão[2], and Icaro Soares[3, *]

Abstract—Nowadays, due to the ever-increasing number of electronic devices and communication systems that use high-frequency electromagnetic waves, a significant level of electromagnetic energy is available in the environment that is not entirely used. In this work, a complete electromagnetic harvesting system using a rectenna is proposed to collect this energy and feed a temperature measurement module. The rectenna is constituted by a combination of a microstrip antenna that captures the electromagnetic energy and a rectifier circuit that converts it into electric energy in direct current (DC) form to feed ultra-low-power loads. The proposed system uses a rectangular microstrip antenna, designed and optimized by using the Computer Simulation Technology (CST®) software to operate at 2.45 GHz. This designed antenna presents a measured reflection coefficient lower than −20 dB at the operating frequency with a maximum gain equal to 7.26 dB. In addition, a voltage doubler rectifier circuit is designed and optimized by using the Advanced Design System (ADS®) to match the impedance of the designed antenna to reduce the reflection losses between these two modules, achieving maximum measured efficiency of approximately 33%. Furthermore, a boost converter circuit is designed for the power management between collected and delivered powers to the sensor and to provide appropriate voltage levels to feed the temperature measurement module. This module consists of an ultra-low-power microcontroller and a temperature sensor that operates in the range of 1.8–3.6 V. The procedures for designing and testing each module of this system are detailed. Finally, a prototype is built and tested under different operating conditions to confirm its functionality and feasibility. These tests show that the proposed system can operate without batteries, only with the harvested electromagnetic energy dispersed in the environment, even from modulated and pulsating sources, as is the case of commercial routers.

1. INTRODUCTION

At present, there is a great demand for the development of systems that use energy more efficiently and for new sources of energy, even if destined to feed small loads. In this context, the concept of energy harvesting is applied using different sources, such as near electromagnetic field [1, 2], solar [3], piezoelectric [4], and Seebeck effect [5].

In addition to the ongoing energy demand, the expansion of technologies and services that operate wirelessly — such as mobile phones, WiFi routers, and television stations — have made available a considerable energy density in the environment, in the form of electromagnetic waves, which is not being fully consumed. Within this context, a new technology has been investigated with the purpose of harvesting this energy to feed low-power loads. This technology is called Electromagnetic Energy Harvesting System (EEHS), and its basic element is the rectenna, which is essentially the combination

Received 9 June 2021, Accepted 3 August 2021, Scheduled 10 August 2021

* Corresponding author: Icaro Soares (icaro.soares@ieee.org).

[1] Department of Electric Engineering, Federal Center for Technological Education of Minas Gerais, Belo Horizonte, Brazil. [2] Department of Electric Engineering, Federal University of Minas Gerais, Belo Horizonte, Brazil. [3] Institut d'Électronique et des Technologies du Numérique, Université de Rennes 1, Rennes, France.

of an antenna with a rectifier circuit [6–8]. The former is responsible for capturing the electromagnetic signals present in the environment, while the latter aims to convert the signal from alternating current into direct current (DC). This DC signal is used, for example, to supply low consumption loads, especially those requiring mobility, and those employed in the application of the Internet of Things (IoT) [9, 10] and remote sensing [11, 12].

The foremost rectenna usage challenges for energy harvesting are due to the signal high frequency content and its low levels of power. This low power signal available in the environment minimizes the levels of power delivered to the load, and limits the possibilities of technology use [13]. Thus, different solutions have been investigated with the aim of increasing the ability of the rectenna to deliver more power to the load [14–16].

Therefore, for the design of an operational and efficient EEHS, one must consider the frequency and the power density of the electromagnetic wave available in the environment of its installation. Another significant aspect that should be considered is the inclusion of a circuit to perform the impedance matching between the antenna and the rectifier circuit. The function of this circuit is to ensure the reduction of the number of reflected waves between these two elements and thus increasing the efficiency of the system [17, 18]. Since the EEHS deals with low-level input power, another element that can be added to the system is a boost converter. This converter is capable of raising the voltage level in the load and performing the power management in a storing element, for example, a supercapacitor [19].

Thus, this work aims to develop a theoretical and experimental EEHS for feeding a low-power temperature sensor. In several industrial, medical and laboratory processes, the temperature of fluids and solutions must be constantly monitored and controlled. In this way, due to its technical significance, there are in literature different approaches to tackle this problem efficiently. For instance, the changes in the electromagnetic parameters in liquids have been exploited in order to monitor properties such as temperature [20, 21], humidity [22, 23] and acidity [24]. However, in most industrial processes wired network of all the sensors is costly and constructively difficult, which sometimes makes unfeasible the real-life application of these sensors. Therefore, as some works show [25–27], energy harvesting techniques have a strong potential as a low-cost alternative for powering these ultra-low-power sensors in a remote network. Moreover, the chosen environment in which this paper is focused has signals with frequency content around the 2.45 GHz band, which is justified by the large number of communication devices operating in this band.

In this context, the contribution of this work is to demonstrate an experimental study of the technical feasibility of a low-cost rectenna technology for feeding commercial low-consumption loads, mainly focused on ultra-low-power sensors for fluid monitoring. There are in the literature some works that present the design and application of energy harvesting systems [28–30]. However, in this paper not only the detailed design of each module that composes the proposed rectenna is presented and thoroughly analyzed with simulations and measurements, but also it carries out a careful investigation of the operation of these modules working individually and together, in order to achieve efficient power management from the harvesting of the electromagnetic power dispersed in the environment to the power delivered to the sensor at the output. Besides, the proposed system is highly reproducible, scalable and can be employed in many other applications apart from which this paper is mainly focused.

This work is organized as follows: Section 2 presents the methodology for the EEHS project and the partial results of each module. In Section 3, the results obtained from the complete EEHS are discussed. Section 4 presents the final considerations of this work.

2. ELECTROMAGNETIC ENERGY HARVESTING SYSTEM

In this work, the design, construction, and testing of an EEHS for feeding a temperature monitoring module (MMT) are carried out. This module consists basically of an ultra-low power consumption microcontroller and a temperature sensor. The block diagram of Fig. 1 shows the EEHS under analysis. The operation frequency was chosen to be at 2.45 GHz once it is a frequency in the Industrial, Scientific and Medical (ISM) band in which many communication devices also operate. In particular, WiFi routers that operate in this frequency can be ubiquitously found in urban areas, which increases the power level in this specific band. Moreover, this frequency allows the miniaturization of the designed system, assuring a reasonable antenna efficiency. For these reasons, the 2.45 GHz band is one of the

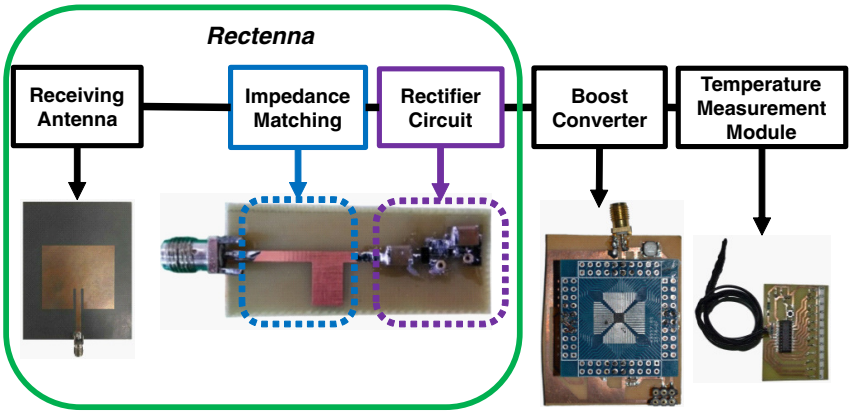

Figure 1. Block diagram of the proposed EEHS.

most used for energy harvesting applications [31].

The design of an EEHS requires the preliminary analysis of the power and frequency of the electromagnetic waves available in the environment. This concern has the purpose of increasing the efficiency of the EEHS and harvesting as much energy as possible from the environment.

2.1. Antenna Design

The antenna configuration chosen to compose the rectenna of this work is the rectangular microstrip type, which offers an easy construction. The topology of the antenna projected is shown in Fig. 2(a) and its surface current distribution in Fig. 2(b).

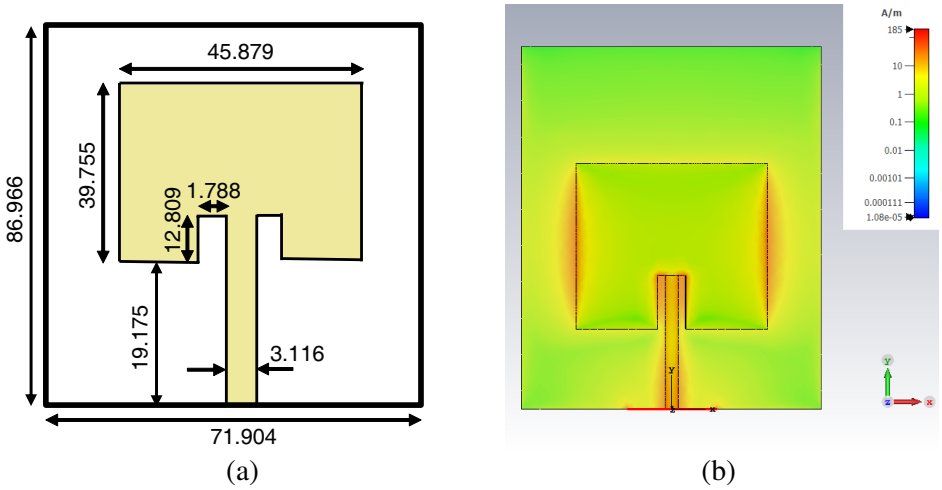

Figure 2. Rectangular microstrip antenna with recess: (a) topology and dimension (in mm) and (b) surface current distribution at 2.45 GHz.

The dielectric substrate used is Rogers RT/Duroid® 5880 (relative electrical permittivity $\varepsilon_r = 2.2$, loss tangent $\delta = 0.0009$ and thickness $h = 1.57$ mm) covered on both sides by copper plates (thickness $t = 0.035$ mm). The antenna dimensions, initially calculated according to [32], are optimized by using the Genetic Algorithm technique available in Computer Simulation Technology (CST®) software, aiming to achieve the lowest value of parameter S_{11} at the frequency of 2.45 GHz, and the results are presented in Fig. 2(a).

Using the dimensions obtained from the optimization process, two prototypes are constructed.

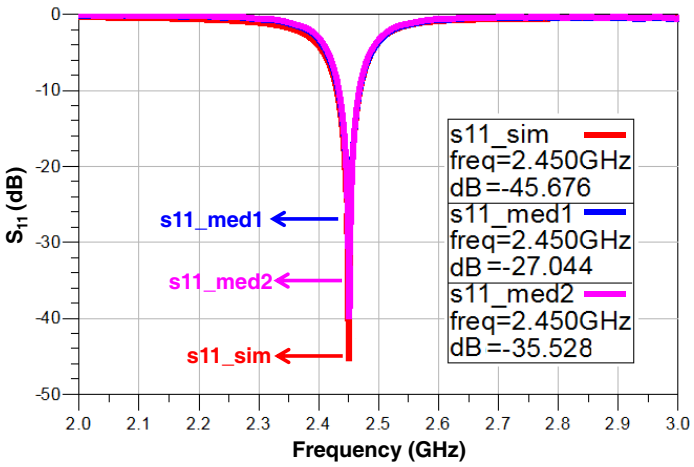

Figure 3. Simulated and measured parameters S_{11} for the rectangular microstrip antenna: s11_med1 (transmitting antenna) and s11_med2 (receiving antenna) indicate the measured values and s11_sim the simulated value.

The simulated and measured results of the S_{11} parameter are depicted in Fig. 3. As can be observed, these results are very close, which validates the optimization and construction of the antennas. The prototypes are operational since they present $S_{11} < -10\,\text{dB}$ at the 2.45 GHz frequency. It should be emphasized that all S_{11} measurements are performed using the Anechoic Chamber DST200 (Rohde & Schwarz®) and the E5071C network analyzer (Keysight®).

The tridimensional radiation pattern for the designed antenna is presented in Fig. 4(a), and its farfield properties are indicated in Fig. 4(b). As it can be seen, at 2.45 GHz, the maximum gain for this antenna is 7.26 dB with Half Power Beam Width (HPBW) of 78°, First Null Beamwidth (FNBW) of 315°, Front-to-Back ratio (F/B) of 28.9°, and Side Lobe Level (SLL) equal to 26°.

The antennas prototypes are also tested in a set up in which one operates as a transmitting and another as receiving antenna. The transmitting antenna is connected to the N5181A high frequency signal generator (Keysight®) set to operate at the frequency of 2.45 GHz and to provide a power of

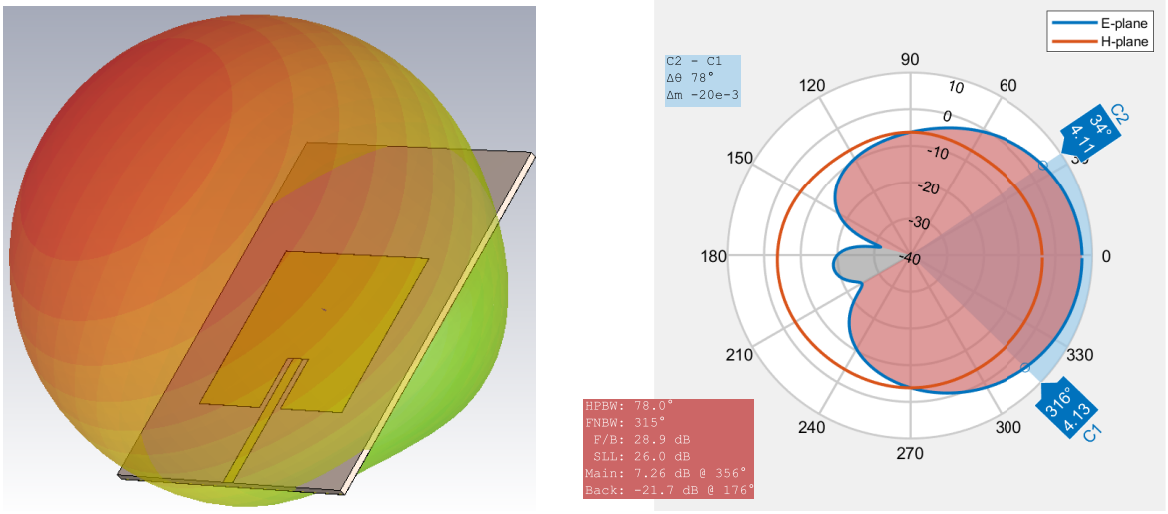

(a) (b)

Figure 4. Radiation pattern for the designed patch antenna at 2.45 GHz: (a) tridimensional plot and (b) E-plane and H-plane plots with indicated farfield properties.

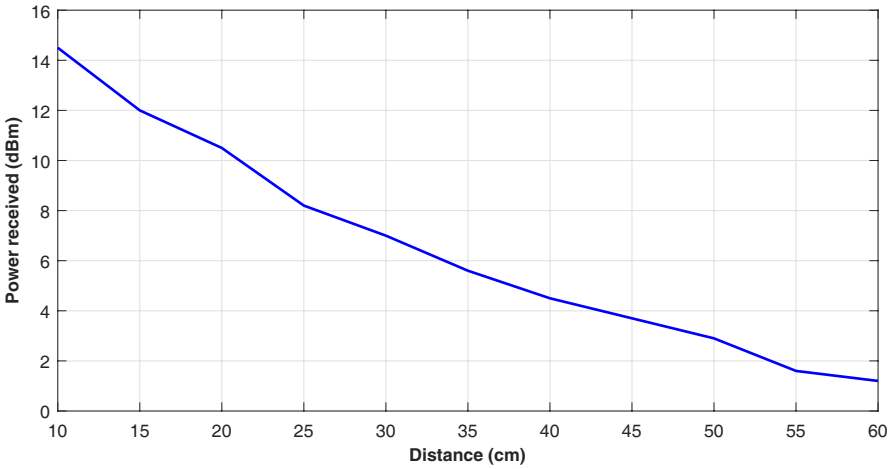

Figure 5. Power received (dBm) by the receiving antenna vs distance between the antennas.

26 dBm. The receiving antenna is connected to the FieldFox® N9912A spectrum analyzer (Keysight®) to measure the power received from different distances set between the antennas. The results obtained are shown in Fig. 5. As it can be observed, the power level received by the receiving antenna decreases with increasing of the distance, presenting values close to 1 dBm at the largest tested distance (60 cm).

2.2. Design of the Rectifier Circuit

The proper choice of topology as well as electronic components to be used is fundamental for the design of an efficient rectifier circuit to compose a rectenna. In addition, one must take into account the characteristics of the signal to be delivered to the rectifier circuit through the antenna.

The rectifier circuit topology adopted in this work is the voltage doubler, whose diagram is illustrated in Fig. 6. This topology is simple since it uses few electronic components, and it is able to raise the voltage level delivered to the load. In order to perform the rectification, the HSMS2862 is used, which includes two Schottky diodes encapsulated at the same integrated circuit. They are capable to operate at 2.45 GHz and present a low barrier voltage (250 to 350 mV). In spite of these advantages, the Schottky diode presents a non-linear behavior as a function of the frequency and the power of the input signal [14], which is taken into account in the design of the rectifier circuit.

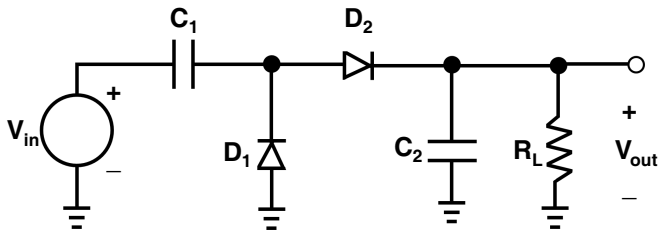

Figure 6. Diagram of the voltage doubler type rectifier circuit.

The boost converter connected to the MMT is modeled using a 3.01 kΩ resistor load (R_L). The capacitance values C_1 and C_2, both equal to 100 µF, are selected to better adjust to the pulsating profile of the router signal (source of the electromagnetic energy to be harvested). Open stub configuration performs the impedance matching. This choice is done because of its constructive simplicity and its outstanding performance, without the use of discrete components.

The geometry dimensions of the rectifier circuit were simulated and optimized using the Advanced Design System (ADS®) software. The LSSP (Large-Signal S-Parameter Simulation) tool is adopted

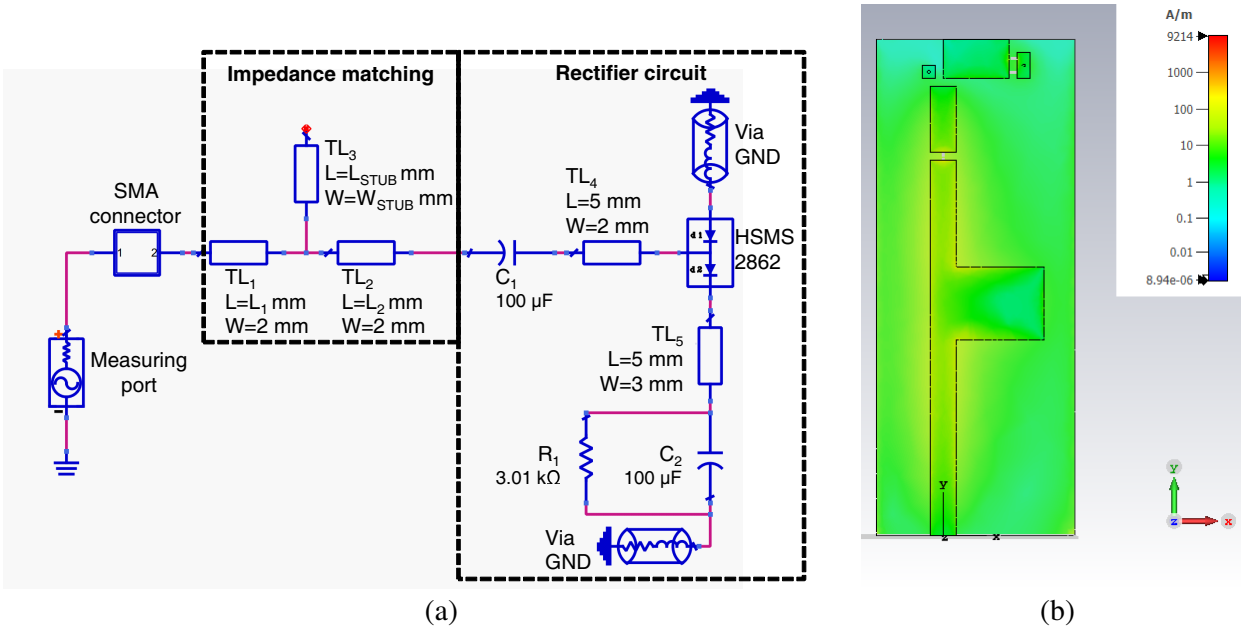

Figure 7. Rectifier circuit: (a) topology (TL = microstrip transmission line, L = length of TL, and W = thickness of TL) and (b) surface current distribution at 2.45 GHz.

because it is suitable for the circuit simulations including non-linear components, such as the HSMS2862 diode. The optimization process schematic is illustrated in Fig. 7(a).

The SMA connector has the function of performing the interface between the circuit and the measuring equipment, and its influence is also considered in the simulation. The dimensions of the impedance matching circuits (L_1, L_2, L_{STUB} and W_{STUB}) are optimized using the random optimization method to achieve two objectives with the same importance:

- Setting the input impedance value of the rectifier, Z_{in}, at 50 Ω in the frequency range 2.4–2.5 GHz. The input power (P_{input}) was set at 0 dBm;
- Acquiring the maximum value of S_{11} equal to −10 dB for P_{input} ranging from 0 to 10 dBm and fixed frequency at 2.45 GHz.

These frequency and power ranges have been chosen to ensure that the rectifier is feasible in an environment that has WiFi internet signals, and considering the result shown in Fig. 5. The rectifier circuit is optimization is done by considering its construction on an FR-4 substrate ($\varepsilon_r = 4.3$, $\delta = 0.01$ and thickness $h = 1.50$ mm) covered on both sides by copper foils (thickness $t = 0.03$ mm). The fixed dimensions are shown in Fig. 7(a). The optimization process leads to the following values for the free dimensions: $L_1 = 17.603$ mm, $L_2 = 10.796$ mm, $L_{\mathrm{STUB}} = 8.644$ mm and $W_{\mathrm{STUB}} = 5.545$ mm. Fig. 7(b) shows the surface current distribution in the impedance matching and rectifier circuit obtained by the full-wave simulation carried out in CST®.

The optimized rectifier is manufactured and tested for functionality and efficiency. In this test, the prototype is connected via a KLC® SMA3011 connector to the N5181A signal generator, which is adjusted to provide a fixed signal frequency at 2.45 GHz with output power (input power of the rectifier, P_{input}) ranging from −10 to 25 dBm. A multimeter is connected to the load terminals to measure the voltage (V_{out}) value in R_L. The results obtained are presented in the graph of Fig. 8(a), which confirm the operation of the rectifier circuit. Also, it shows the growth of V_{out} with increasing of P_{input} until 17 dBm, where V_{out} begins to stabilize. The efficiency, η, of the rectifier circuit is calculated from the measured values of V_{out} and P_{input}. Fig. 8(b) shows that the maximum value of η achieved by the rectifier circuit is approximately 33% for $P_{\mathrm{input}} = 17$ dBm. From circuit analysis, it can be shown that the maximum theoretical efficiency for this rectifier's topology is approximately 40%; therefore, the measured efficiency is close to this limit. The main factors that reduced this efficiency are the

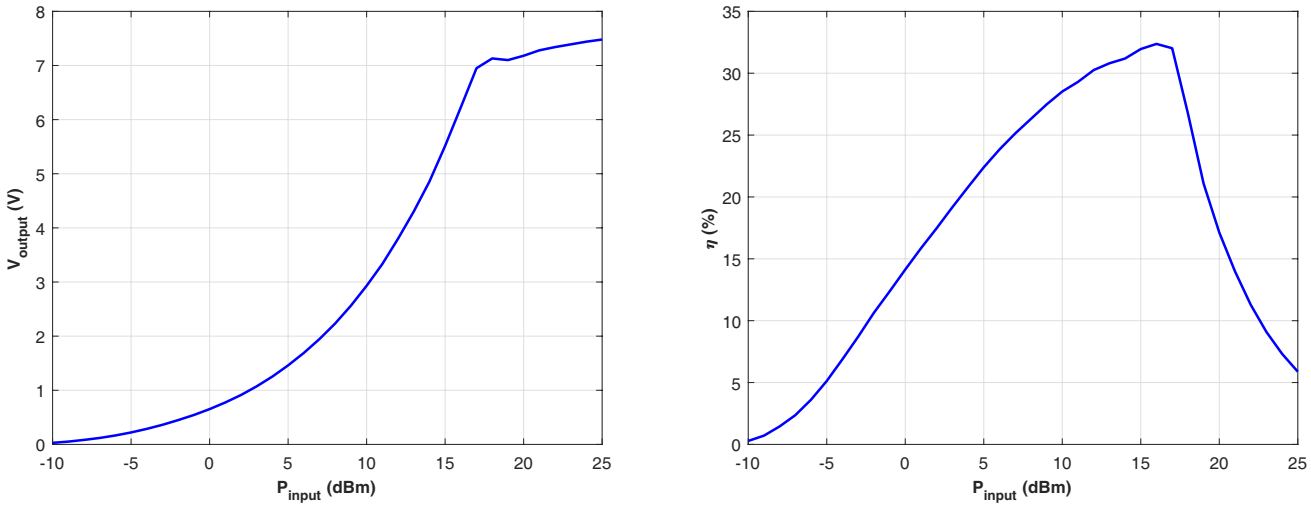

Figure 8. Rectifier circuit performance as a function of the input power: (a) Output voltage (V_{output}) and (b) efficiency (η).

non-idealities of the commercial electronic devices and their losses. In addition, it changes the input impedance of the circuit, increases the reflection losses in the prototype. One alternative to mitigate this effect is to design an adaptive impedance matching circuit capable of matching the rectifier impedance considering the non-idealities and fluctuations in the input power.

2.3. Boost Converter Design

The output available by the EEHS may not be sufficient to power the MMT, and there is no guarantee that the available power in the environment is constant. Hence, it is convenient to employ a boost converter and energy storage elements, such as capacitors or supercapacitors. The converter has the function of raising the voltage level at the rectenna output and also performing the energy management of the EEHS. The BQ25504, manufactured by Texas Instruments®, has been selected to be part of the EEHS under analysis because it has low starting voltage, low power consumption, ability of storing energy by supercapacitor (ensuring that the power supplied to the load is constant, even with the variation of the input power) and protection circuit against under and overvoltage.

The BQ25504 is programmed by choosing the value of external resistors. The value of these components depends on the specific requirements of each application. For the EEHS under study, these requirements are presented in Table 1. The calculation follows the methodology provided by the device

Table 1. Project requirements for BQ25504 converter.

Parameter	Value
Voltage Range for Overvoltage Threshold (VBAT_{OV})	3.5 V
Voltage Range for Under Voltage Threshold (VBAT_{UV})	2.2 V
Voltage Range for Threshold Voltage for High to Low Transition of Digital Signal Indicating Battery is OK (VBAT_{OK})	2.4 V
Voltage Overvoltage Hysteresis Thresold ($\text{VBAT}_{\text{HYST}}$)	2.8 V
MPPT (Maximum Power Point Tracker)	disabled
Digital Programming Input for IC over Temperature Threshold (OT)	65°C

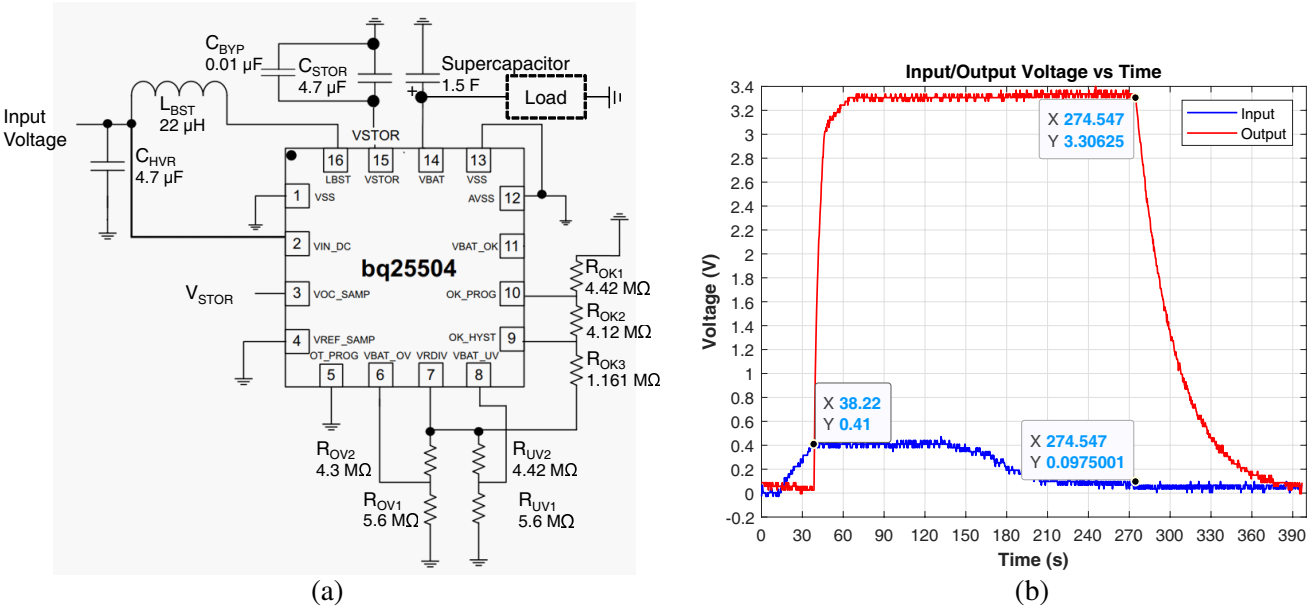

Figure 9. Boost converter: (a) schematic, and (b) voltage profile obtained in the boost converter test.

manufacturer. The pin diagram of the converter is shown in Fig. 9(a), together with the calculated resistors.

The prototype constructed of the circuit presented in Fig. 9(a) is submitted to a test focused on determining the level of voltage in which the converter starts its operation. Also, once operating, it is determined what is the minimum voltage that guarantees the operation of the converter. To perform this test, the variable voltage source E3631A (Keysight®) is connected to the drive input. The two channels of the DSO7032A oscilloscope (Keysight®) are connected to the input and output of the converter, respectively. A 100 kΩ resistor is used as a load at the converter output, and a 470 µF capacitor is used as the energy storage element. These values are chosen so that the constant RC of the circuit allows a better visualization of the output signal behavior. The results of this test are shown in Fig. 9(b).

Initially, the value of the input voltage of the circuit is changed from 0 V to the value needed to make the converter go into operation. It has been verified that the converter starts operating when the voltage at its input reaches at least 441 mV. Afterwards, the input voltage value is reduced to the value at which the converter shuts down. It has been found that, once in operation, the converter maintains its operation for input voltage values greater than 97.5 mV. In addition, the boost converter is able to maintain the output voltage level by approximately 3.3 V, even under variations at the input voltage of the circuit.

2.4. Design of the Temperature Monitoring Module

This section presents the design of a module for temperature monitoring, which demonstrates the potential of using the EEHS. The MMT consists of a temperature sensor connected to the ultra-low power consumption microcontroller (µC) MSP430G2132. It has the function of processing the measured temperature information and displaying it in the LEDs temperature scale connected to its outputs. There is a total of twelve LEDs, graduated with 5°C each, starting from 5°C to 60°C, as shown in Fig. 10.

The MSP430 family is suitable microcontrollers for low power supply applications, likewise the EEHS case. Its low consumption is due to the standby mode operation that works most of the time. In addition to this main feature, the MSP430G2132 meets the other requirements needed for the proposed application, which are: operation with low voltage supply (the MSP430G2132 is capable of working with voltages between 1.8 to 3.6 V), having a channel analog-digital converter (ADC) and containing digital outputs to display the measured temperature on the LEDs.

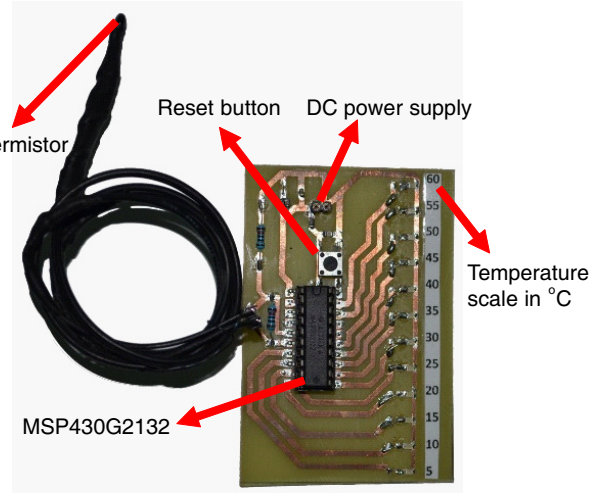

Figure 10. Prototype of the temperature monitoring module.

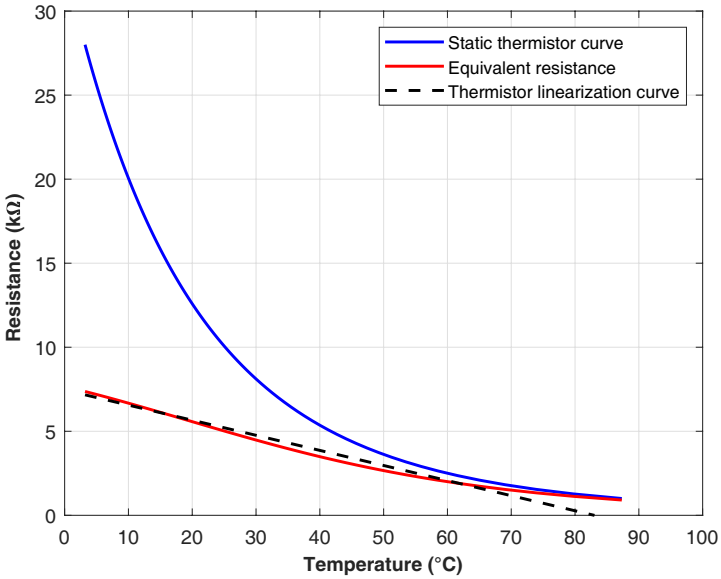

Figure 11. Behavior of the NTC thermistor resistance, equivalent resistance and linearization vs temperature.

The operating modes of the MSP430G2132 are shown as alternatives to combine performance with low power consumption. Besides the active mode (AM), there are five low-power modes (LPM) options. In this work, μC is programmed using AM and LPM3 modes. The AM mode is required for the CPU to process the contents of the interrupts (reading the digital-analog converter and processing the on/off LEDs logic). The LMP3 mode is selected because it consumes low energy and, at the same time, it allows the timer operation.

The temperature sensor chosen to compose the MMT is the 10 kΩ NTC thermistor because it has high input resistance, high sensitivity and the possibility of operation with low voltage values. However, this sensor presents non-linear resistance behavior as a function of the temperature, described by Eq. (1), known as Steinhart & Hart equation, which is shown in Fig. 11 (blue thermistor static curve):

$$\frac{1}{T+273} = 1.13 \times 10^{-3} + 2.34 \times 10^{-4} \ln(R) + 8.81 \times 10^{-9} [\ln(R)]^3 \quad (1)$$

where T is the temperature in °C, and R is the thermistor resistance, given in Ω. The coefficients of

Eq. (1) are obtained by means of the calibration of the thermistor using a digital thermometer with a measuring range between −50°C and 110°C.

The MSP430G2132 is not able to handle calculations involving logarithms and exponentials. Since the response curve of the thermistor is logarithmic in its nature, it is necessary to linearize the sensor for the correct temperature reading. Therefore, the thermistor curve is linearized by inserting a 10 kΩ resistor in parallel with the thermistor. Fig. 11 shows, in addition to the static curve, the equivalent resistance curve and the curve linearized from the Eq. (2).

$$R = -89.817 \times T + 7455.4 \tag{2}$$

From the graph obtained in Fig. 11, it is possible to observe that the linearization process by the parallel resistor insertion technique is satisfactory. It reduces the resistance variation, especially at lower temperatures, and it makes possible the proper interpretation of measurements by the microcontroller. On the other hand, the linearization process carried out reducing the sensor sensitivity.

3. RESULTS AND DISCUSSIONS

The antenna, the rectifier circuit, the boost converter, and the MMT are interconnected to form the EEHS. Two tests are performed to verify the functionality of the system. In both tests, a capacitor of 470 µF is connected to the boost converter, to perform energy storage. This value is chosen to reduce the test period since the use of supercapacitors would require a few hours for its complete discharge.

The first test, called energy reuse test (R-test), consists in connecting one of the antenna prototypes (transmitting antenna) to the TP-Link® WR841HP router, tuned to channel 9 (2.452 GHz), with peak power of 18 dBm. The EEHS is positioned at 30 cm from the transmitting antenna. In the second test, called the wireless energy transmission test (T-test), it is possible to provide higher power levels for the EEHS and, thus, greater distances between the source and the EEHS are achieved. This test is performed to demonstrate the potential of the technology by using a source of high frequency signals with the power greater than the source used in the R-test and dedicated exclusively to the power supply of the EEHS. In the T-test, the N5181A signal generator is connected to the transmitting antenna and configured to provide a 26 dBm signal at the 2.45 GHz fixed frequency, and the EEHS is positioned at 1.90 m from the transmitting antenna. Fig. 12 shows the block diagram of the tests performed. Figs. 14 and 15 show the experimental assemblies of R and T tests, respectively.

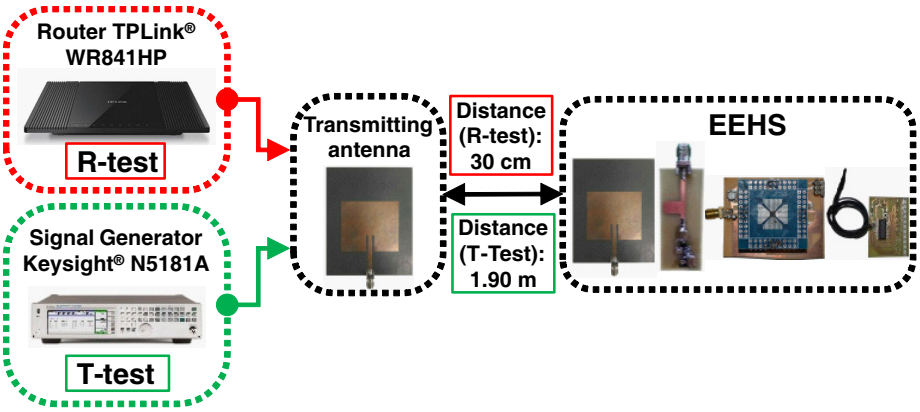

Figure 12. Block diagram of the R-test and T-test.

The R-test was run for thirty minutes with the setup shown in Fig. 13, monitoring the temperature in a cold and hot liquid. By changing the position of the temperature sensor from the hot liquid to the cold one, the temperature LED display gradually reduced its temperature degree (due to thermistor inertia) ranging from 45°C to 10°C. It is noteworthy that the objective of this work is not to measure strictly the temperature, but rather, to demonstrate the viability of the technology under study to feed low consumption sensors. It is important to emphasize the use of the boost converter because the signal

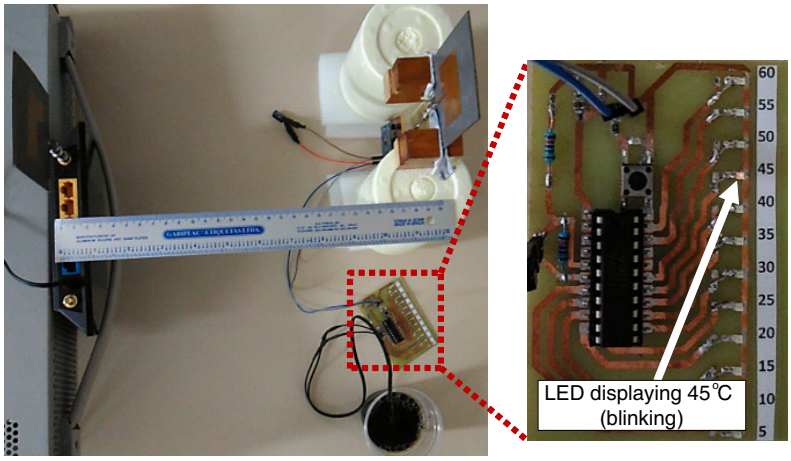

Figure 13. Experimental setup of the R-test, where the MMT is magnified.

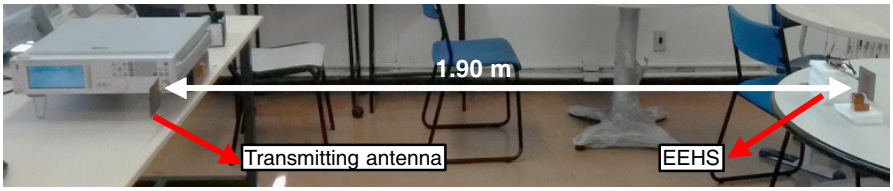

Figure 14. Experimental setup of the T-test.

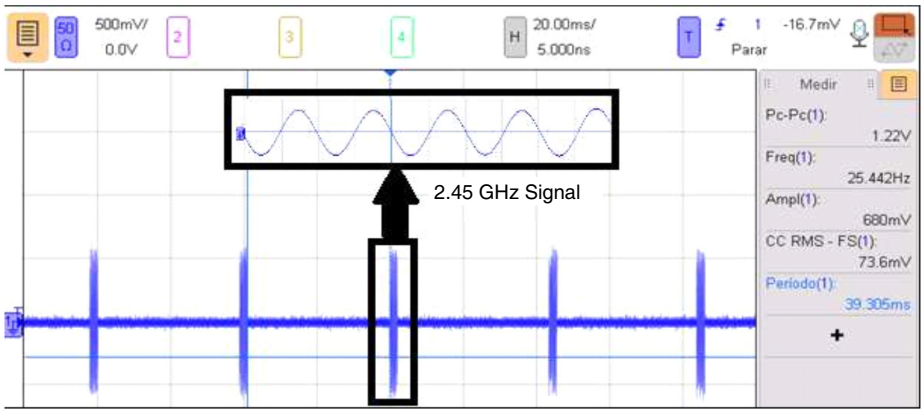

Figure 15. Signal measured at the output of the TP-Link® WR841HP router.

provided by the router is pulsating, as shown in Fig. 15. Thus, the absence of the boost could imply in commutation between on and off states of the microcontroller since the capacitors used in the rectifier circuit are not large enough to hold the value of the voltage at the load.

The T-test was performed for one hour, under the conditions shown in Fig. 14. Temperature monitoring was also performed on a cold liquid and a hot liquid. It should be noted that the signal supplied by the N5181A generator does not have the same characteristics as the signal shown in Fig. 15. In this case, the signal is a sine wave oscillating at 2.45 GHz and not a pulsating signal, thus providing a higher average power level to the test.

According to the tests performed in this Section, it is possible to check the functionality of the designed system for both energy harvesting and power transmission. Even using a high-power

commercial router, the maximum distance reached for the proper operation of the system was 30 cm in the R-test. This value is considerably smaller when compared to the T-test, which reached a distance of 1.90 m. This fact is due to the use of the signal generator, which is capable of providing higher power and a non-pulsed signal. Thus, the T-test demonstrates the potential of the technology because if a higher power commercial router were used, longer distances would be reached.

With the results obtained, the application of the designed EEHS is recommended for monitoring the environmental parameters where the exchange of batteries can be a limiting factor, as in areas of difficult access. It is noteworthy that a set of antennas and rectifier associations was not used in this work, which could increase the power delivered to the load as presented in [14] since it was chosen by the EEHS compaction.

The EEHS can be designed for operation in other frequency bands as well as in multi-frequencies since current commercial routers can operate in the 2.4 GHz and 5.8 GHz bands. To operate at 5.8 GHz band, a new rectenna design should be performed because both the antenna and the rectifier were designed specifically for the 2.4 GHz band. However, the MMT would not undergo any modification because its power is in direct current. Thus, it is verified that the EEHS presents flexibility since it is possible to adapt the rectenna to the MMT according to the environment to be monitored.

4. CONCLUSION

In this work, a low-cost and easily reproducible system for electromagnetic energy harvesting, using rectenna, applied to the temperature monitoring was proposed, systematically described, designed and analyzed through simulations and measurements. Even though this paper focused its application on remote fluid temperature monitoring for industrial processes, the same device could also be applied for other kinds of ultra-low-power sensors that can be found in agriculture [33], medicine [34], domotics [35], among other applications.

The proposed system is composed of a rectangular microstrip antenna with a measured reflection coefficient lower than -20 dB at the operating frequency of 2.45 GHz that was chosen once many communication devices operate in this ISM band, and consequently the level of electromagnetic power dispersed in the environment at this frequency is substantial. This antenna also presents a maximum gain equal to 7.26 dB with a half-power beamwidth of 78°. In order to convert the power collected by this antenna to a DC power, a half-wave rectifier was designed and optimized to match the antenna's impedance and thus mitigate the losses due to reflection. The efficiency measured for this rectifier was around 33% which is closer to the maximum theoretical efficiency for this rectifier's topology. Then, a boost converter was designed to carry out the power management and assure that the voltage level delivered to the sensor is between 1.8 and 3.6 V. Finally, the load for this system is constituted by an ultra-low-power sensor and microcontroller unit responsible for processing the measured data.

A prototype for this system was built and tested for both harvesting and wireless power transmission. In both tests, it was found that the technology is feasible and functional to power sensors with low power consumption. For wireless transmission, it is possible to achieve greater distances (1.9 m) between the transmitting and receiving antenna, since the signal emitted is dedicated exclusively to this type of application. In turn, harvesting energy has the characteristic of dealing with environmental signals that have low power and presents a variable frequency and power, making the impedance matching between the antenna and the rectifier more complex. Besides that, the dispersed signal is modulated and pulsating, which becomes reduces the harvest power level. However, the built prototype is capable of operating even in this situation. Finally, through the results obtained, it is possible to conclude that the proposed system is feasible in practice and demonstrates that the electromagnetic energy presented in the environment is able to feed low consumption loads.

ACKNOWLEDGMENT

The authors thank the Conselho Nacional de Desenvolvimento Científico e Tecnológico (CNPq), Coordenação de Aperfeiçoamento de Pessoal de Nível Superior (CAPES) and Fundação de Amparo à Pesquisa do Estado de Minas Gerais (FAPEMIG) for the financial support received for the development of this work.

REFERENCES

1. Shinohara, N., "Trends in wireless power transfer: WPT technology for energy harvesting, mllimeter-wave/THz rectennas, MIMO-WPT, and advances in near-field WPT applications," *IEEE Microwave Magazine*, Vol. 22, No. 1, 46–59, 2021.
2. Gonçalves, Y., U. Resende, and I. Soares, "Electromagnetic energy harvesting using a glass window," *Journal of Microwaves, Optoelectronics and Electromagnetic Applications*, Vol. 19, No. 1, 50–59, 2020.
3. Hamied, F. M. A., K. Mahmoud, M. Hussein, and S. S. A. Obayya, "Design and analysis of rectangular spiral nano-antenna for solar energy harvesting," *Progress In Electromagnetics Research C*, Vol. 111, 25–34, 2021.
4. Wu, N., B. Bao, and Q. Wang, "Review on engineering structural designs for efficient piezoelectric energy harvesting to obtain high power output," *Engineering Structures*, Vol. 235, 112068, 2021.
5. Shakeel, M., K. Rehman, S. Ahmad, M. Amin, N. Iqbal, and A. Khan, "A low-cost printed organic thermoelectric generator for low-temperature energy harvesting," *Renewable Energy*, Vol. 167, 853–860, 2021.
6. Brown, W. C., "The history of power transmission by radio waves," *IEEE Transactions on Microwave Theory and Techniques*, Vol. 32, No. 9, 1230–1242, 1984.
7. Divakaran, S., D. Krishna, Nasimuddin, and J. K. Antony, "Dual-band multi-port rectenna for RF energy harvesting," *Progress In Electromagnetics Research C*, Vol. 107, 17–31, 2021.
8. Pandey, R., A. K. Shankhwar, and A. Singh, "An improved conversion efficiency of 1.975 to 4.744 GHz rectenna for wireless sensor applications," *Progress In Electromagnetics Research C*, Vol. 109, 217–225, 2021.
9. Sanislav, T., G. D. Mois, S. Zeadally, and S. C. Folea, "Energy harvesting techniques for internet of things (IoT)," *IEEE Access*, Vol. 9, 39530–39549, 2021.
10. Okba, A., A. Takacs, and H. Aubert, "Compact flat dipole rectenna for IoT applications," *Progress In Electromagnetics Research C*, Vol. 87, 39–49, 2018.
11. Dong, Y., P. Fan, and K. B. Letaief, "Energy harvesting powered sensing in IoT: Timeliness versus distortion," *IEEE Internet of Things Journal*, Vol. 7, No. 11, 10897–10911, 2020.
12. Xu, H., L. Tsang, J. Johnson, K. C. Jezek, J.-B. Yan, and P. Gogineni, "A combined active and passive method for the remote sensing of ice sheet temperature profiles," *Progress In Electromagnetics Research*, Vol. 167, 111–126, 2020.
13. Williams, A., M. Torquato, I. Cameron, A. Fahmy, and J. Sienz, "Survey of energy harvesting technologies for wireless sensor networks," *IEEE Access*, Vol. 9, 77493–77510, 2021.
14. Brandão, G. L. F., Ú. C. Resende, F. S. Bicalho, G. A. T. Almeida, and M. M. Afonso, "Parallel association of rectennas for electromagnetic energy harvesting," *Proceedings of the 18th International Symposium on Electromagnetic Fields in Mechatronics, Electrical and Electronic Engineering*, 2017.
15. Pereira, P., R. C. M. Pimenta, R. Adriano, G. L. F. Brandão, and Ú. C. Resende, "Antenna impedance correction for low power energy harvesting devices," *Proceedings of the SBMO/IEEE MTT-S International Microwave and Optoelectronics Conference*, 2017.
16. Corrêa, D. C., U. C. Resende, F. S. Bicalho, and Y. S. Gonçalves, "Design, optimization and experimental evaluation of a F-shaped multiband metamaterial antenna," *J. Microwaves, Optoelectron. Electromagn. Appl.*, Vol. 17, No. 4, 590–603, 2018.
17. Li, S., F. Cheng, C. Gu, S. Yu, and K. Huang, "Efficient dual-band rectifier using stepped impedance stub matching network for wireless energy harvesting," *IEEE Microwave and Wireless Components Letters*, Vol. 31, No. 7, 921–924, 2021.
18. Liu, L., Q.-Y. Xiang, D. Tian, and Q. Feng, "A novel antenna feeding network with separately resonant frequency and impedance matching tunable capability," *Progress In Electromagnetics Research Letters*, Vol. 81, 85–91, 2019.

19. Wagih, M., N. Hillier, S. Yong, A. Weddell, and S. Beeby, "RF-powered wearable energy harvesting and storage module based on E-textile coplanar waveguide rectenna and supercapacitor," *IEEE Open Journal of Antennas and Propagation*, Vol. 2, 302–314, 2021.
20. Altıntaş, O., M. Aksoy, E. Ünal, M. Karaaslan, and C. Sabah, "Operating frequency reconfiguration study for a split ring resonator based microfluidic sensor," *Journal of the Electrochemical Society*, Vol. 167, No. 14, 147512, 2020.
21. Chakravartula, V., S. Rakshit, S. Dhanalakshmi, R. Kumar, and R. Narayanamoorthi, "Linear temperature distribution sensor using FBG in liquids — Local heat transfer examination application," *IEEE Sensors Journal*, 2021.
22. Dalgaç, S., M. Furat, M. Karaaslan, O. Akgöl, F. Karadağ, M. Zile, and M. Bakir, "Grease oil humidity sensor by using metamaterial," *Journal of Electromagnetic Waves and Applications*, Vol. 34, No. 18, 2488–2498, 2020.
23. Yu, H., C. Wang, F. Meng, J. Xiao, J. Liang, H. Kim, S. Bae, D. Zou, E. Kim, N. Kim, M. Zhao, and B. Li, "Microwave humidity sensor based on carbon dots-decorated MOF-derived porous Co_3O_4 for breath monitoring and finger moisture detection," *Carbon*, 2021.
24. Lin, L., W. Jiang, X. Xu, and P. Xu, "A critical review of the application of electromagnetic fields for scaling control in water systems: Mechanisms, characterization, and operation," *NPJ Clean Water*, Vol. 3, No. 1, 2021.
25. Ma, K., Z. Li, P. Liu, J. Yang, Y. Geng, B. Yang, and X. Guan, "Reliability-constrained throughput optimization of industrial wireless sensor networks with energy harvesting relay," *IEEE Internet of Things Journal*, 2021.
26. Lee, W., H. Park, S. Kim, S. Park, D. Kim, and H. Lee, "Wireless-powered VOCs sensor based on energy-harvesting metamaterial," *Advanced Electronic Materials*, Vol. 7, No. 5, 2001240, 2021.
27. Abdulkarim, Y., H. Awl, F. Alkurt, F. Muhammadsharif, S. Saeed, M. Karaaslan, M. Bakır, and H. Luo, "A thermally stable and polarization insensitive square-shaped water metamaterial with ultra-broadband absorption," *Journal of Materials Research and Technology*, Vol. 13, 1150–1158, 2020.
28. Cai, X., W. Geyi, and Y. Guo, "A compact rectenna with flat-top angular coverage for RF energy harvesting," *IEEE Antennas and Wireless Propagation Letters*, Vol. 20, No. 7, 1307–1311, 2021.
29. Lu, P., C. Song, and K. Huang, "Ultra-wideband rectenna using complementary resonant structure for microwave power transmission and energy harvesting," *IEEE Transactions on Microwave Theory and Techniques*, Vol. 69, No. 7, 3452–3462, 2021.
30. Roy, S., R. Tiang, M. Roslee, M. Ahmed, and M. Mahmud, "Quad-band multiport rectenna for RF energy harvesting in ambient environment," *IEEE Access*, Vol. 9, 77464–77481, 2021.
31. Gu, X., L. Grauwin, D. Dousset, S. Hemour, and K. Wu, "Dynamic ambient RF energy density measurements of montreal for battery-free IoT sensor network planning," *IEEE Internet of Things Journal*, doi: 10.1109/JIOT.2021.3065683, 2021.
32. Balanis, C. A., *Antenna Theory — Analysis and Design*, 2nd Edition, John Wiley & Sons, Hoboken, NJ, 1997.
33. Morais, R., J. Mendes, R. Silva, N. Silva, J. Sousa, and E. Peres, "A versatile, low-power and low-cost IoT device for field data gathering in precision agriculture practices," *Agriculture*, Vol. 11, No. 7, 619, 2021.
34. Sowmya, N., S. Rout, and R. Patjoshi, "Implementation of ultra-low-power electronics for biomedical applications," *Electronic Devices, Circuits, and Systems for Biomedical Applications*, 153–176, 2021.
35. Stolojescu-Crisan, C., C. Crisan, and B. Butunoi, "An IoT-based smart home automation system," *Sensors*, Vol. 21, No. 11, 3784, 2021.